
STRUCTURE AND PROPERTIES
OF THE DEFORMED STATE

Plastic Deformation of Piezoelectric Lanthanum–Gallium Tantalate Crystals during Cyclic Mechanical Actions

O. M. Kugaenko^{a,*}, S. S. Uvarova^a, V. S. Petrakov^b, O. A. Buzanov^c, V. N. Egorov^c,
S. A. Sakharov^c, and M. L. Pozdnyakov^d

^aNational University of Science and Technology MISiS, Leninskii pr. 4, Moscow, 119049 Russia

*e-mail: crystalXXI@isis.ru

^bEconomic Power Institute, Moscow, 117587 Russia

^cOAO Fomos-Materials, Moscow, 107023 Russia

^dTsNII KM Prometei, St. Petersburg, 191015 Russia

Received October 18, 2011

Abstract—The microstructure of piezoelectric lanthanum–gallium tantalite single crystals is shown to change substantially during cyclic mechanical actions at room temperature and during thermal shock: the dislocation density increases, twinning takes place, and a mesostructure forms. This effect is related to the appearance of piezoelectric fields, which significantly decrease the temperature of the onset of plastic deformation of these brittle single crystals, during mechanical actions.

DOI: 10.1134/S0036029513040071

1. INTRODUCTION

Langasite $\text{La}_3\text{Ga}_5\text{SiO}_{14}$ (LGS) is the most known lanthanum–gallium silicate: it was first synthesized early in the 1980s [1, 2]. Lanthanum–gallium tantalite $\text{La}_3\text{Ga}_{5.5}\text{Ta}_{0.5}\text{O}_{14}$ (LGT) is an isomorph of langasite and a promising piezoelectric. Single-crystal LGT elements are used as sensitive piezoelectric elements in pressure, vibration, and temperature sensors that can operate over a wide temperature range (up to 1000°C). As compared to the traditional materials (piezoelectric ceramics, quartz) applied in physical quantity sensors, LGT single crystals have the following advantages: thermally stable piezoelectric characteristics, absent pyroelectric effect, and no phase transformations up to the melting temperature (1450°C). The efficiency of using LGT crystals is also related to a high electromechanical coupling coefficient (which is almost threefold that of quartz), which makes it possible to create piezoelectric elements operating due to the direct piezoelectric effect.

The piezoelectric elements in the transducers in internal combustion engines undergo extreme sign-alternating loads (both mechanical and thermal), and their fracture occurs because of fatigue. The change in the state of a material during a fatigue process is known to be reflected on its mechanical properties and a macro- and microstructure. It should be noted that the fatigue strength of metals and alloys was studied in numerous monographs and works. However, the rather expensive elements that are made of brittle

materials, namely, dielectric and semiconductor crystals and ceramics, and operate under sign-alternating load conditions are widely used in modern engineering. The behavior of brittle crystals during cyclic loading is poorly understood, and the working capacity of an element cannot be predicted without allowance for the mechanisms of its fracture and the causes of degradation of its structure and properties.

The investigation of the laws of fracture of langasite family crystals during uniaxial compression did not reveal plastic deformation in them up to $0.9T_m$, which was determined as the brittle–ductile transition temperature in [3]. Therefore, to study the fatigue and fracture of such brittle materials as LGT single crystals during cyclic loading is a challenging problem. The purpose of this work is to analyze the deformation mechanisms of LGT single crystals and the laws of their fracture under thermal and sign-alternating load conditions.

2. EXPERIMENTAL

We studied LGT single crystals (trigonal symmetry class 32). The model of the LGT structure is shown in Fig 1. Langasite crystals form as layers located normal to the [0001] crystallographic direction [4]. The structure of LGT has no cleavage plane and exhibits a strong anisotropy of properties.

The LGT single crystals were grown according to the Czochralski method in OAO Fomos-Materials

along the $[11\bar{2}0]$ direction, the crystal weight was 3.5 kg, and the cylindrical part diameter was 80 mm [5, 6]. Samples in the form of plates and cubes whose planes were oriented along axes x , y , and z were cut from the single crystals, and the sample surfaces were mechanically polished.

The anisotropy of the mechanical properties of the initial single crystals was estimated by measuring the Vickers microhardness and microbrittleness on a Tukon 2100V microhardness tester at a load of 0.25 N.

We also determined critical stress (fracture toughness) intensity factor K_{Ic} , which is the cracking resistance criterion for a material. For the case of indentation by a Vickers pyramid, we calculated K_{Ic} by the formula [7]

$$K_{Ic} = 0.035(L/a)^{-1/2}(\mu E/H_v)^{2/5}H_v a^{1/2} \mu^{-1},$$

where L is the radial crack length (m), a is the indentation half-width (m), μ is the Poisson ratio, E is Young's modulus (Pa), and H_v is the microhardness (Pa).

The fatigue strength of the LGT crystals was studied at room temperature during cyclic sign-alternating loading via compression of samples in the form of $1 \times 1 \times 1$ -cm cubes and $1 \times 1 \times 0.2$ -cm plates of various crystallographic orientations when a load was applied along axes x , y , and z . For this purpose, we used a high-frequency pulsator with an Amsler 20 HFP 5100 (Zwick/Roell) electromagnetic resonance driver. The tests were carried out up to $N = 10^6$ loading cycles. A static load was applied by compression at a stress of 5–150 MPa, and the dynamic load was 1–100 MPa. The maximum load range was 200 MPa, which corresponded to $0.5\sigma_u$ (σ_u is ultimate tensile strength) of crystals at room temperature [3]. The resonance load cycling frequency (100–150 Hz) depended on the loading conditions, and a change in this frequency was used to detect the fracture time of a sample.

The thermal resistance of the LGT single crystals was estimated using thermal shock upon water (25°C) quenching of samples heated to 100–1000°C. The samples consisted of x -cut workpieces for pressure piezoelectric sensors, i.e., thin mechanically polished 0.2-mm-thick plates with an outside diameter of 6–15 mm and an inside diameter of 3–6 mm. They were heated in a furnace to a given temperature for 20 min and were then water cooled.

Internal thermomechanical stresses σ_{in} in the LGT crystals during thermal shock were calculated by the well-known Kingeri formula, which makes it possible to determine internal thermal stresses in materials during quenching at a cooling rate of 10^6 K/s,

$$\sigma_{in} = \frac{E\alpha(T_2 - T_1)}{(1 - \mu)},$$

where E is the elastic modulus of LGT ($\parallel Z$, 190 GPa; $\perp Z$, 110 GPa), μ is the Poisson ratio, T_2 is the sample

Table 1. Angular characteristics of the rocking curves of LGT crystals

Reflection (hkl)	Reflection angle	Intensity half-width	Maximum width of reflection curve
(2240)	22°51'	7.5''	0°2'24''
(3030)	19°30'	8.6''	0°5'24''
(0004)	37°55'	10.5''	0°2'24''

heating temperature (100–1000°C), T_1 is the cooling water temperature (25°C), and α is the linear thermal expansion coefficient (TEC).

The TEC used in the calculations was measured for the LGT crystals in various crystallographic directions in air in the temperature range 20–700°C upon heating at a rate of 5 K/min in a LINSEIS 76/1000 dilatometer.

Since LGT is an active piezoelectric, its compression results in the direct piezoelectric effect with the formation of electric field E_i along the loading direction. The piezoelectric fields appearing in LGT crystals during mechanical actions were calculated by the formula

$$E_i = -g_{ijk}\sigma_{jk},$$

where g_{ijk} are the piezoelectric coefficients (third-order tensor components) and σ_{jk} is the mechanical stress applied to the sample. The piezoelectric moduli and stress coefficients along x in LGT crystals are $d_{11} = -6.5 \times 10^{-12}$ C/N and $g_{11} = -38 \times 10^{-3}$ (V m)/N [8]. Piezoelectric modulus d_{11} in an LGT crystal remains constant in the temperature range up to 600°C.

X-ray diffraction (XRD) studies of the pole figure recorded with a Bruker D8 diffractometer equipped with a Bruker scintillation detector showed that all samples in the initial state were single crystals free of twins and other defects.

Rocking curves were recorded with a D8 Advance (Bruker, Germany) high-resolution X-ray diffractometer at six points in each sample at a step of 3 mm using $CuK_{\alpha 1}$ radiation. The scale along the y axis is logarithmic. As a quantitative scattering characteristic, we chose the reflection curve half-width, which is equal to the angular width of a diffraction profile at the intensity equal to half maximum. The investigation results averaged over six points are presented in Fig. 2 and Table 1.

The half-width of the rocking curves of polished LGT samples did not exceed 9"–12", which indicates a high degree of structural perfection and a high quality of surface finishing.

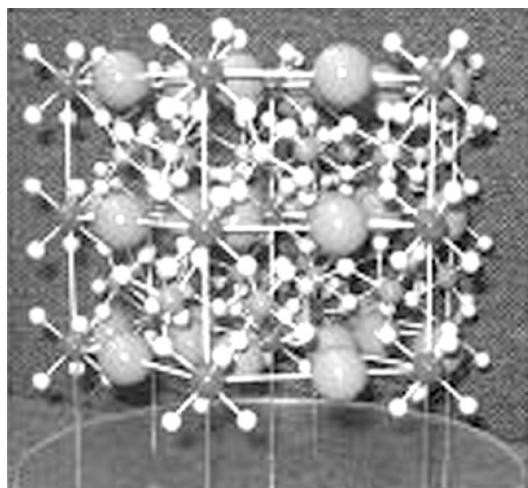


Fig. 1. Spatial model for langasite family crystals.

The microstructures of the initial crystals and those subjected to cyclic deformation and thermal shock were revealed by selective etching in an $\text{HCl} : \text{HNO}_3 = 1 : 1$ solution and were analyzed with a microscope. The dislocation density calculated from etching pits and averaged over 10 fields of view in a crystal plane in the initial samples was 10^4 cm^{-2} .

3. RESULTS AND DISCUSSION

3.1. Microhardness and Cracking Resistance

The results of calculating the microhardness and the cracking resistance coefficient along various crystallographic directions in the LGT crystals are given in Table 2. As in [9], we revealed an anisotropy of second-kind hardness: the microhardnesses of the $[0001]$, $[10\bar{1}0]$, and $[11\bar{2}0]$ sections are different with an anisotropy coefficient of 1.2. Obviously, the anisot-

Table 2. Microhardness H_v and stress intensity factor K_{Ic} of LGT crystals

Crystallographic orientation of sample (hkl)	H_v , GPa	K_{Ic} , $\text{MPa m}^{-1/2}$
$(10\bar{1}0)$	10.08	0.88
$(11\bar{2}0)$	10.22	0.91
(0001)	8.77	1.16

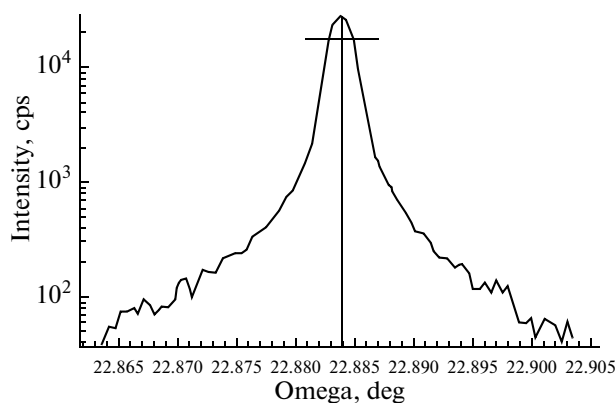


Fig. 2. Angular characteristics of the rocking curves of LGT crystals; $(22\bar{4}0)$ reflection.

ropy of second-kind hardness in the LGT crystals is related to different reticular densities of the faces and to the bonds in them.

Along with the anisotropy of hardness, the LGT crystals are also characterized by the anisotropy of microbrittleness. The fracture toughness anisotropy coefficient is 1.3; that is, cracking along the $[11\bar{2}0]$ and $[10\bar{1}0]$ surfaces occurs easier than on the $[0001]$ surface at the same load. In this case, harder surfaces have lower values of K_{Ic} (Table 2), which corresponds to similar studies of other materials [7].

3.2. Endurance

LGT crystal plates withstand 3×10^5 loading cycles with the formation of visible cracks upon the application of a static compression load of 5–10 MPa or a dynamic load of 2–5 MPa. The change in the loading frequency did not exceed 1 Hz; that is, the sample stiffness remained almost the same during cyclic loading. When the static load increased to 20 MPa at a dynamic load of 5 MPa, the resonance frequency increased during the entire test (Fig. 3). This indicates a gradual change in the sample stiffness because of a change in the sample microstructure. The loading frequency changes jumpwise during fracture and is related to a sharp decrease in the crystal stiffness, i.e., the appearance of a main crack, individual microcracks, and spalls.

Cubic samples withstand 3×10^5 loading cycles without the formation of visible cracks during axisymmetric cyclic compression loading at a load of 10–15 MPa along the x , y , and z axes at a frequency of 100–150 Hz and room temperature. As the load or the number of loading cycles increases, samples fail, in most cases, via cracking along the $[11\bar{2}0]$ and $[10\bar{1}0]$

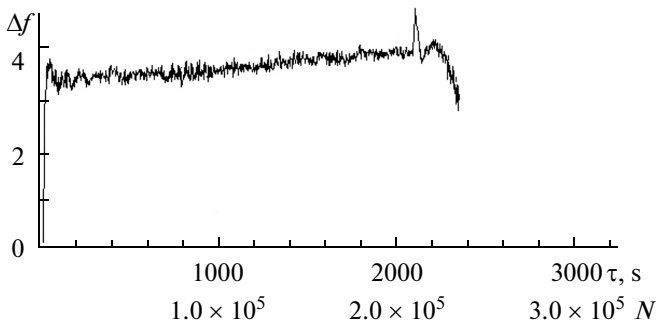


Fig. 3. Change in the loading cycle frequency Δf vs. test time τ and the number of loading cycles N of LGT plates.

planes (Fig. 4), which corresponds to the cracking resistance data.

The fracture surfaces formed upon cyclic loading have a complex river structure with a high dislocation density induced by high stresses in the samples (Fig. 5). The development of a dislocation structure during cyclic loading begins in the near-surface layer, which has the minimum shear stability in a loaded crystal. Therefore, plastic flow in the near-surface layer begins earlier and develops more intensely as compared to the material volume.

The necessity of the compatibility of the deformations of the plastically deformed near-surface layer and the elastically loaded volume causes the development of a deformation mesoscopic substructure in the near-surface layer. At low strains ($N = 10^4 - 10^5$ cycles) and low loads (static load of 1 kN, dynamic load of 0.5 kN), a mesoscopic structure with a cell size of about 10 μm forms on the sample surface at room temperature (Fig. 6). At medium strains ($N = 10^5 - 10^6$ cycles), a system of localized deformation mesobands forms along the directions of the maximum shear stresses.

3.3. Thermal Stability

The thermal stresses that appear during thermal shock upon water quenching lead to a change in the microstructure of the single-crystal LGT samples and to their fracture with crack formation. After quenching from a temperature below 120°C, the samples do not undergo fracture and the dislocation density increases to 10^8 cm^{-2} . This finding supports the mechanism of defect and dislocation formation during the relaxation of the thermal stresses induced by quenching. Quenching from a temperature above 200°C causes numerous cracking events, and cracks propagate in a direction close to $[11\bar{2}0]$ in all samples (Fig. 7). Slow cooling of crystals from 1000°C in 1 day relieves stresses in a crystal and results in a decrease in the dislocation density below the initial value.

XRD analysis shows that thermal shock from a temperature of 220°C causes additional reflections,

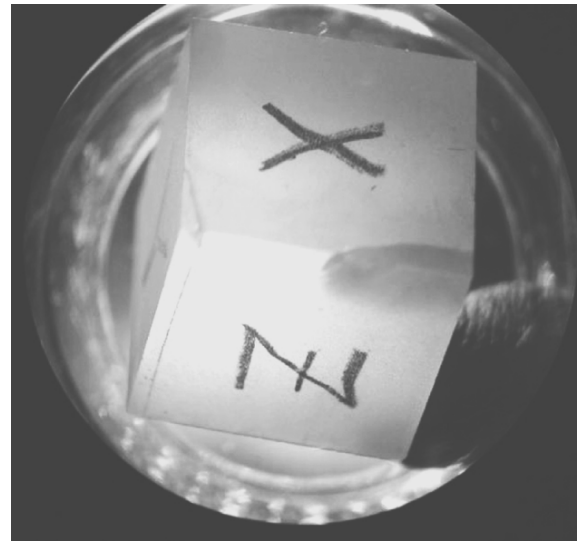


Fig. 4. Fracture surface of an LGT sample ($10 \times 10 \times 10 \text{ mm}$) with a crack that is parallel to the y -cut plane after cyclic tests at room temperature, a static load of 2 kN, a dynamic load of 0.5 kN, and $N = 2 \times 10^5$ loading cycles.

which make an angle of 60° to the center of the pole figure, in the (1000) pole figure. The appearance of these reflections during thermal shock is related to twinning along the $(11\bar{2}0)$ plane.

Thus, the application of cyclic mechanical stresses (whose amplitude is lower than the ultimate tensile strengths of the crystals) and shock thermal loads at

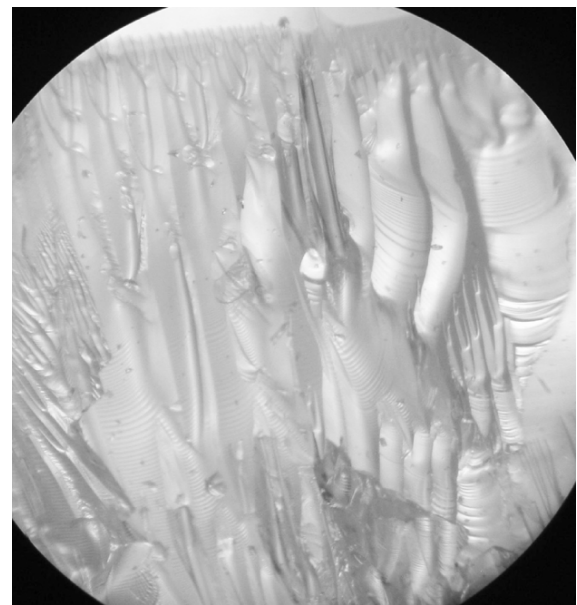


Fig. 5. River pattern on the cleavage surface of an LGT crystal after cyclic actions when the load was increased from 2 to 15 kN.

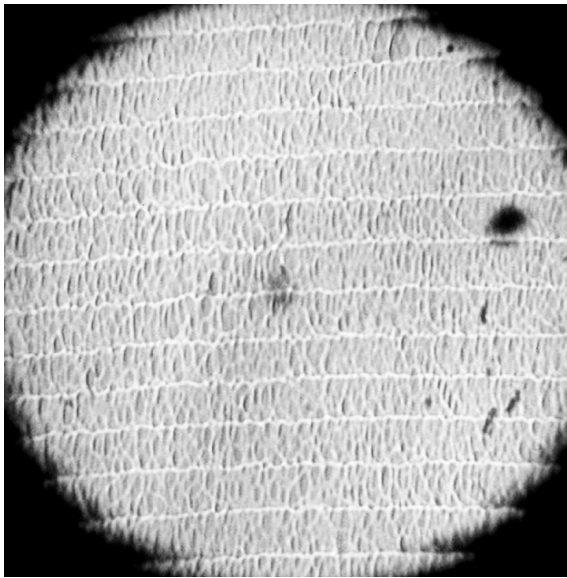


Fig. 6. Mesostructure of a brittle LGT crystal, $\times 300$.

room temperature cause a significant change in the microstructures of the LGT crystals, which is associated with an increase in the dislocation density (which increases by 4–5 orders of magnitude as compared to the initial density), twinning, and the formation of the mesostructure characteristic of ductile metals [10]. This change in the structure indicates the manifestation of the plasticity effect in brittle piezoelectric LGT crystals, which is in conflict with the generally accepted concepts of absent plastic deformation in LGT at room temperature. The detected effect was analyzed with allowance for the piezoelectric properties of the LGT crystals. The piezoelectric activity is maximal in x -cut samples along the x axis, and the piezoelectric effect is absent in z -cut samples along the z axis.

According to the calculation results, the internal thermomechanical stresses in the LGT crystals during thermal shock in the course of water quenching from temperatures up to 200°C are below the yield strengths of the crystals (Table 3), and these stresses upon quenching from 400°C or above exceed the ultimate tensile strength of the crystals upon brittle fracture determined in [3] and are considered to be unacceptable. The internal stresses appearing during thermal shock (60–1300 MPa) cause a potential difference of 20–400 kV/cm (due to the piezoelectric effect) in the compression direction on the opposite sides of an LGT sample (see Table 3). These high mechanical and electric fields lead to microcrack nucleation, an increase in the dislocation density, and fracture of the crystals.

The calculation of the direct piezoelectric effect during cyclic loading showed that the electric fields

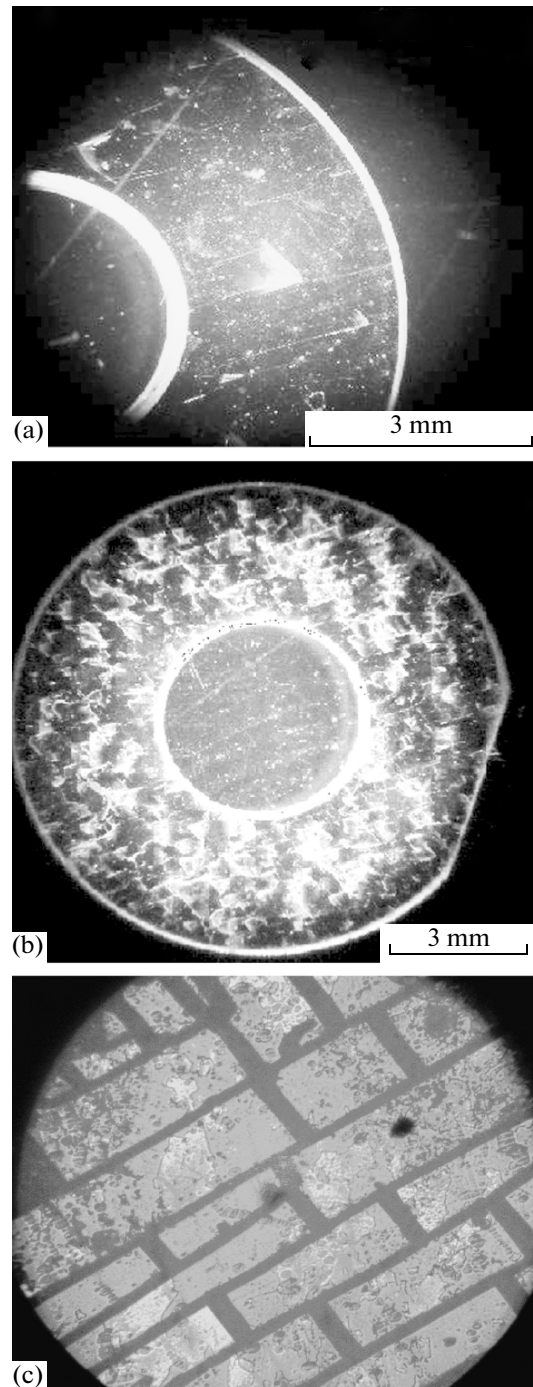


Fig. 7. Samples quenched from a temperature of (a) 200°C ($\times 12$), (b) 300°C ($\times 7$), and (c) 300°C ($\times 100$).

can reach 70 kV/cm on the opposite sides of an x -cut LGT plate at a stress amplitude up to 200 MPa. An ac electric field with a frequency equal to the frequency of a mechanical action appears in a crystal during cyclic loading. This field decreases the energy of dislocation breakaway from pinning centers and changes the microstructure of a crystal.

Table 3. Internal thermal stresses σ_{in} in LGT during thermal shock, thermal expansion coefficient α , and quenching-induced piezoelectric fields E (with respect to axis z)

$\Delta T, ^\circ\text{C}$	$\alpha \times 10^{-6}, 1/^\circ\text{C}$		σ_{in}, MPa		$E, \text{kV/cm}$
	α_{33}	α_{11}	$\parallel Z$	$\perp Z$	$\perp Z$
75	4.5	6.25	81.7	65.7	24
175	5	6.75	212	166	62
275	5.25	7.25	349	279	106
375	5.3	7.55	481	397	150
475	5.4	7.75	621	516	196
575	5.5	7.95	765	641	243
675	5.6	8	915	757	287
775	5.6	8	1050	869	330
875	5.6	8	1190	981	372

Note: $\Delta T = T_2 - T_1$, where T_2 is the sample heating temperature and T_1 is the cooling water temperature (25°C).

CONCLUSIONS

(1) When brittle lanthanum–gallium tantalite single crystals are subjected to cyclic loading and thermal shock at loads well below their yield strength, their microstructure changes substantially: the dislocation density increases by 3–4 orders of magnitude as compared to the initial state, twinning takes place, and a mesostructure forms. The crystals fail mainly via cracking along the x and y planes, which agrees with the anisotropy of microbrittleness of the crystals.

(2) As follows from the calculation of the direct longitudinal piezoelectric effect, the electric field reaches 70 kV/cm on the opposite sides of x -cut LGT samples subjected to cyclic loading at a stress amplitude up to 20 kN/cm². This field results in a decrease in the cracking threshold in the crystals, restructuring of the dislocation structure in them, twinning, and a significant decrease in the temperature of the onset of plastic deformation in the brittle crystals.

(3) The results of investigation of the mechanical properties of the crystals demonstrate that LGT crystals are promising materials under sign-alternating mechanical and thermal loading, where the level of

sign-alternating loads reaches 20 kN/cm² at a frequency of 100–150 Hz. The LGT crystals withstood thermal shocks upon quenching at a temperature difference of 120–150°C, and quenching at a larger temperature difference results in fracture of the crystals.

ACKNOWLEDGMENTS

This work was supported by the Federal Science and Innovation Agency (state contract no. 02.523.11.3013).

REFERENCES

1. B. V. Mil', A. V. Butashin, and A. M. Ellern, "Germanates with the $\text{Ca}_3\text{Ga}_2\text{Ge}_4\text{O}_{14}$ structure," *Izv. Akad. Nauk SSSR, Neorg. Mat.* **19** (10), 1715–1717 (1983).
2. B. V. Mill and Yu. V. Pisarevsky, "Langasite-type materials: from discovery to present state," in *Proceedings of International Conference 2000 IEEE/EIA*, pp. 133–144.
3. A. M. Aronova, G. V. Berezhekova, A. V. Butashin, and A. A. Kaminskii, "Strength and ductility of $\text{La}_3\text{Ga}_5\text{SiO}_{14}$ single crystals," *Kristallografiya* **35** (4), 933 (1990).
4. G. M. Kuz'micheva, O. Zakharko, E. A. Tyunina, et al., "Point defects in langatate crystals," *Kristallografiya* **54** (2), 303–306 (2009).
5. O. A. Buzanov, "Method for growing lanthanum–gallium silicate single crystals," RF Patent 2108417, *Byul. Izobret.*, 1998, no. 10, p. 3.
6. G. G. Koziov, "Method of preparing a charge for growing lanthanum–gallium silicate single crystals," RF Patent 2126063, *Byul. Izobret.*, 1998, no. 4, p. 3.
7. V. K. Grigorovich, *Hardness and Microhardness of Metals* (Nauka, Moscow, 1976).
8. J. Stade, L. Bonaty, M. Hengst, and R. B. Heimann, "Electrooptic, piezoelectric, and dislocation properties of langasite ($\text{La}_3\text{Ga}_5\text{SiO}_{14}$), langataite ($\text{La}_3\text{Ga}_{5.5}\text{Ta}_{0.5}\text{O}_{14}$), langanite ($\text{La}_3\text{Ga}_{5.5}\text{Nb}_{0.5}\text{O}_{14}$)," *Cryst. Res. Technol.* **37** (10), 1113–1120 (2002).
9. O. A. Buzanov, O. M. Kugaenko, and T. N. Ovcharenko, "Anisotropy of the mechanical properties of brittle complex oxide crystals," in *Proceedings of XIII National Conference on Crystal Growth NKRK-2008* (Moscow, 2008), p. 256.
10. V. E. Panin, "Physical mesomechanics of the surface layers of solids," *Fiz. Mezomekh.* **2** (6), 5–23 (1999).

Translated by K. Shakhlevich

SPELL: 1. ok